

Comparative study of CO₂ adsorption in a series of zeolites

Loïc Bénariac-Doumal^{1,a}, Irena Deroche^{2,3}, Habiba Nouali^{2,3}, Jean-Louis Paillaud^{2,3}, Taylan Ors², Andrew N. Fitch¹ and Catherine Dejoie^{1,a}

¹ European Synchrotron Radiation Facility, 71 avenue des Martyrs 38000 Grenoble, France

² Université de Haute Alsace, IS2M, 15 rue Jean Starcky 68057 Mulhouse, France

³ Université de Strasbourg 67000 Strasbourg, France

^a loic.benariac@orange.fr; catherine.dejoie@esrf.fr

Structural description

Table S1: Refinement results for CO₂@Si-STT

Pressure (bar)	No. of CO ₂ molecules (puc)	a (Å)	b (Å)	c (Å)	β (°)	Volume (Å ³)	Distances Si-O (Å)	Angles O-Si-O (°)	Angles Si-O-Si (°)	Rwp	Rp	Rexp
0	0	13.12121(4)	21.75469(7)	13.71238(4)	102.51250(18)	3821.20(2)	1.572(8)-1.651(8)	108.7(4)-110.2(4)	135.0(5)-171.0(4)	6.167	6.225	1.410
1.25	2.79(3)	13.12359(4)	21.75549(7)	13.70843(4)	102.51732(19)	3820.87(2)	1.577(9)-1.650(8)	108.8(4)-110.2(4)	134.7(5)-169.3(5)	6.279	6.138	1.399
1.5	3.34(3)	13.12373(4)	21.75540(7)	13.70783(4)	102.51815(19)	3820.71(2)	1.573(9)-1.653(9)	108.7(4)-110.2(5)	135.0(6)-169.1(5)	6.262	6.081	1.394
1.75	3.83(3)	13.12394(4)	21.75550(7)	13.70731(4)	102.5191(2)	3820.63(2)	1.576(9)-1.650(8)	108.8(4)-110.2(5)	134.7(6)-169.4(5)	6.302	6.054	1.387
2	4.45(3)	13.12415(4)	21.75536(7)	13.70664(4)	102.5204(2)	3820.46(2)	1.578(9)-1.649(8)	108.8(4)-110.2(5)	134.5(6)-169.5(5)	6.328	6.011	1.393
2.5	5.27(3)	13.12442(5)	21.75566(8)	13.70613(5)	102.5222(2)	3820.42(2)	1.575(9)-1.651(9)	108.7(5)-110.2(5)	134.8(6)-169.3(5)	6.476	6.101	1.394
3	6.12(3)	13.12486(5)	21.75623(8)	13.70562(5)	102.5249(2)	3820.47(2)	1.577(9)-1.649(9)	108.7(5)-110.2(5)	134.6(6)-169.4(5)	6.574	6.103	1.384
3.5	7.15(3)	13.12555(5)	21.75730(8)	13.70540(5)	102.5283(2)	3820.74(2)	1.571(10)-1.653(10)	108.7(5)-110.2(5)	135.0(6)-169.2(6)	6.738	6.168	1.379
4	7.91(4)	13.12617(5)	21.75842(8)	13.70537(5)	102.5323(2)	3821.06(3)	1.576(10)-1.649(10)	108.8(5)-110.2(5)	134.6(6)-169.7(6)	6.901	6.275	1.376
5	8.73(4)	13.12705(5)	21.75974(9)	13.70550(5)	102.5372(2)	3821.51(3)	1.573(11)-1.651(10)	108.7(5)-110.2(5)	134.8(7)-169.4(6)	7.047	6.328	1.376
7.5	9.79(4)	13.12871(6)	21.76241(9)	13.70601(6)	102.5456(3)	3822.48(3)	1.577(11)-1.649(11)	108.8(6)-110.2(6)	134.6(7)-169.8(6)	7.306	6.450	1.372
10	10.59(4)	13.13045(6)	21.76460(10)	13.70662(6)	102.5525(3)	3823.43(3)	1.577(11)-1.649(11)	108.8(6)-110.2(6)	134.5(7)-169.9(6)	7.484	6.557	1.366
12.5	11.02(4)	13.13154(6)	21.76587(10)	13.70672(6)	102.5579(3)	3823.92(3)	1.568(12)-1.655(12)	108.7(6)-110.2(6)	135.2(8)-169.1(7)	7.617	6.653	1.362
15	11.29(4)	13.13254(6)	21.76695(10)	13.70699(6)	102.5619(3)	3824.42(3)	1.574(12)-1.650(11)	108.7(6)-110.2(6)	134.7(8)-169.6(7)	7.671	6.637	1.356
20	11.75(4)	13.13387(6)	21.76860(10)	13.70733(6)	102.5663(3)	3825.13(3)	1.574(12)-1.650(12)	108.7(6)-110.2(6)	134.8(8)-169.5(7)	7.817	6.755	1.349

Table S2: Refinement results for CO₂@Si-CHA

Pressure (bar)	No. of CO ₂ molecules (puc)	a (Å)	c (Å)	Volume (Å ³)	Distances Si-O (Å)	Angles O-Si-O (°)	Angles Si-O-Si (°)	Rwp	Rp	Rexp
0	0	13.544354(12)	14.747433(15)	2342.953(5)	1.5906(6)- 1.6110(8)	108.95(6)- 109.78(6)	147.30(9)- 149.84(10)	7.381	4.714	1.355
0.5	1.12(4)	13.544316(12)	14.748070(16)	2343.041(5)	1.5912(6)- 1.6109(9)	108.95(7)- 109.78(7)	147.35(10)- 149.89(11)	7.319	4.649	1.353
2	4.33(3)	13.538547(11)	14.755406(14)	2342.210(4)	1.5897(6)- 1.6113(6)	108.95(7)- 109.78(6)	147.37(10)- 149.95(10)	7.306	4.782	1.336
2.5	5.49(3)	13.537790(12)	14.758353(15)	2342.416(5)	1.5898(6)- 1.6115(6)	108.94(7)- 109.78(6)	147.38(10)- 149.96(11)	7.395	4.941	1.328
3	6.13(3)	13.537716(11)	14.760172(15)	2342.679(5)	1.5896(6)- 1.6116(6)	108.94(7)- 109.79(6)	147.36(10)- 149.95(11)	7.444	4.988	1.370
3.5	6.49(3)	13.537557(11)	14.761220(15)	2342.791(4)	1.5897(6)- 1.6117(6)	108.94(7)- 109.79(6)	147.39(10)- 149.97(11)	7.401	4.996	1.315
4	6.87(3)	13.537621(11)	14.762174(15)	2342.964(4)	1.5896(6)- 1.6119(6)	108.94(7)- 109.78(6)	147.36(10)- 149.95(11)	7.439	5.004	1.316
5	7.39(3)	13.537976(12)	14.763202(16)	2343.250(5)	1.5897(7)- 1.6120(6)	108.94(7)- 109.78(6)	147.37(10)- 149.97(11)	7.507	5.109	1.315
7.5	8.19(3)	13.539404(11)	14.764678(15)	2343.979(5)	1.5898(7)- 1.6124(6)	108.94(7)- 109.78(6)	147.34(10)- 149.94(11)	7.549	5.117	1.306
10	8.66(3)	13.540354(14)	14.765215(17)	2344.393(5)	1.5899(7)- 1.6123(6)	108.94(7)- 109.78(6)	147.34(10)- 149.94(11)	7.684	5.220	1.301
12.5	9.03(3)	13.541427(13)	14.765814(16)	2344.860(5)	1.5901(6)- 1.6126(6)	108.94(6)- 109.78(4)	147.35(10)- 149.94(6)	7.677	5.175	1.295
15	9.22(3)	13.542319(12)	14.766278(16)	2345.243(5)	1.5899(7)- 1.6130(6)	108.94(7)- 109.78(6)	147.33(10)- 149.92(11)	7.680	5.157	1.294
20	9.58(4)	13.543804(13)	14.766656(17)	2345.817(5)	1.5904(7)- 1.6122(6)	108.94(7)- 109.78(6)	147.36(11)- 149.97(12)	7.728	5.215	1.303

Table S3: Refinement results for CO₂@Na-LTA

Pressure (bar)	No. of CO ₂ molecules (puc)	a (Å)	Volume (Å ³)	Distances Si-O (Å)	Distances Al-O (Å)	Angles O-Si-O (°)	Angles O-Al-O (°)	Rwp	Rp	Rexp
0	0	24.57698(6)	14845.19(11)	1.600(6)- 1.611(3)	1.701(6)- 1.711(4)	108.8(3)- 109.8(3)	108.9(3)-110.0(3)	7.198	5.870	2.128
1	19.56(17)	24.55821(5)	14811.19(8)	1.590(6)- 1.616(4)	1.687(6)- 1.716(4)	109.1(3)- 109.6(3)	109.2(3)- 109.8(3)	6.787	5.619	2.363
1.25	22.62(16)	24.55508(4)	14805.53(8)	1.591(6)- 1.613(8)	1.688(6)- 1.709(8)	109.3(3)- 109.55(16)	109.4(3)- 109.6(3)	6.771	5.491	1.910
1.5	26.29(16)	24.55279(5)	14801.39(8)	1.588(6)- 1.616(8)	1.685(6)-1.713(8)	109.3(3)- 109.56(17)	109.4(2)- 109.6(3)	6.984	5.604	1.986
1.75	30.42(17)	24.55126(5)	14798.63(9)	1.589(6)- 1.615(8)	1.686(6)- 1.711(8)	109.3(3)- 109.55(17)	109.4(2)- 109.6(3)	7.110	5.680	2.000
2	34.91(17)	24.55045(5)	14797.17(9)	1.590(6)- 1.614(8)	1.687(6)- 1.710(9)	109.3(3)- 109.55(17)	109.4(2)- 109.6(3)	7.203	5.744	1.989
2.5	38.80(17)	24.55061(5)	14797.45(10)	1.589(7)- 1.615(9)	1.686(7)- 1.712(9)	109.3(3)- 109.55(17)	109.4(2)- 109.6(3)	7.472	5.906	1.987
3	42.63(18)	24.55165(6)	14799.33(10)	1.590(7)- 1.614(9)	1.687(7)- 1.711(9)	109.3(3)- 109.56(17)	109.4(2)- 109.6(3)	7.587	5.972	1.997
3.5	45.05(18)	24.55298(6)	14801.74(10)	1.590(7)- 1.615(9)	1.688(7)- 1.711(9)	109.3(3)- 109.56(18)	109.4(2)- 109.6(3)	7.774	6.104	2.002
4	47.43(18)	24.55452(6)	14804.52(11)	1.589(7)-1.617(10)	1.686(7)- 1.713(10)	109.3(3)- 109.56(18)	109.4(2)- 109.6(3)	7.991	6.078	2.012
5	48.54(18)	24.55629(6)	14807.73(10)	1.589(7)- 1.617(9)	1.687(7)- 1.713(9)	109.3(3)- 109.56(17)	109.4(2)- 109.6(3)	7.954	6.226	2.011
7.5	51.26(18)	24.55917(6)	14812.93(10)	1.590(7)- 1.617(9)	1.687(7)- 1.713(9)	109.3(3)- 109.55(17)	109.4(2)- 109.6(3)	8.057	6.241	2.009
10	52.65(19)	24.56195(6)	14817.97(11)	1.590(7)- 1.617(9)	1.688(7)- 1.713(9)	109.3(3)- 109.56(17)	109.4(2)- 109.6(3)	8.175	6.349	2.009
12.5	53.98(19)	24.56437(6)	14822.35(11)	1.591(7)- 1.616(9)	1.689(7)- 1.712(9)	109.3(3)- 109.56(17)	109.4(2)- 109.6(3)	8.258	6.367	2.012
15	55.30(19)	24.56638(6)	14825.98(11)	1.588(7)- 1.621(9)	1.685(7)- 1.717(9)	109.3(3)- 109.54(17)	109.4(2)- 109.6(3)	8.329	6.412	2.013
20	56.51(19)	24.56885(6)	14830.46(11)	1.592(7)- 1.616(9)	1.689(7)- 1.713(9)	109.3(3)- 109.56(17)	109.4(2)- 109.6(3)	8.329	6.410	2.006

Table S4: Refinement results for CO₂@Na-FAU

Pressure (bar)	No. of CO ₂ molecules (puc)	a (Å)	Volume (Å ³)	Distances T1-O (Å)	Distances T2-O (Å)	Angles O-T1-O (°)	Angles O-T2-O (°)	Rwp	Rp	Rexp
0	0	25.03146(5)	15684.06(10)	1.613(10)- 1.630(7)	1.686(9)- 1.739(8)	108.7(4)- 110.1(5)	109.0(4)- 110.4(3)	6.971	5.326	1.055
2	18.6(4)	25.02031(5)	15663.12(10)	1.615(12)- 1.632(9)	1.688(11)- 1.742(10)	108.7(5)- 110.0(6)	109.0(5)- 110.4(4)	7.689	5.668	1.049
2.5	27.5(3)	25.01058(5)	15644.85(9)	1.613(11)- 1.635(9)	1.685(10)- 1.747(9)	108.7(4)- 109.9(6)	108.9(5)- 110.4(4)	7.480	5.684	1.047
3	39.8(3)	24.99780(5)	15620.88(9)	1.615(8)- 1.627(7)	1.688(8)- 1.738(7)	108.7(4)- 110.0(4)	108.9(4)- 110.5(3)	6.781	5.114	1.038
3.5	52.3(3)	24.99189(5)	15609.81(9)	1.614(7)- 1.627(7)	1.687(8)- 1.738(8)	108.7(4)- 110.0(4)	109.0(4)- 110.5(3)	7.084	5.332	1.028
4	61.4(3)	24.99217(5)	15610.32(9)	1.613(8)- 1.632(6)	1.684(6)- 1.743(7)	108.6(3)- 110.0(4)	108.9(3)- 110.4(3)	6.989	5.302	1.018
5	65.0(3)	24.99436(5)	15614.42(9)	1.612(8)- 1.635(6)	1.681(6)- 1.747(7)	108.6(3)- 109.9(4)	108.9(3)- 110.5(3)	7.056	5.403	1.019
7.5	68.0(3)	24.99756(5)	15620.42(9)	1.614(7)- 1.631(6)	1.685(6)- 1.741(6)	108.7(3)- 110.0(4)	108.9(3)- 110.5(3)	6.980	5.352	1.021
10	70.1(3)	25.00083(5)	15626.55(9)	1.613(7)- 1.636(6)	1.681(6)- 1.748(6)	108.7(3)- 109.9(4)	108.9(3)- 110.4(3)	7.031	5.408	1.021
12.5	71.2(3)	25.00390(5)	15632.32(9)	1.614(7)- 1.633(6)	1.685(6)- 1.744(6)	108.7(3)- 110.0(4)	108.9(3)- 110.5(3)	7.026	5.463	1.019
15	73.3(3)	25.00650(5)	15637.18(9)	1.615(6)- 1.628(6)	1.687(6)- 1.738(6)	108.6(3)-110.0(4)	108.9(3)- 110.5(3)	7.039	5.444	1.013
20	72.6(3)	25.00961(5)	15643.02(9)	1.613(10)- 1.635(8)	1.684(8)- 1.746(8)	108.7(4)- 110.0(5)	108.9(4)- 110.5(3)	7.342	5.592	1.003

T1: Si/T2: 0.9Al:0.1Si

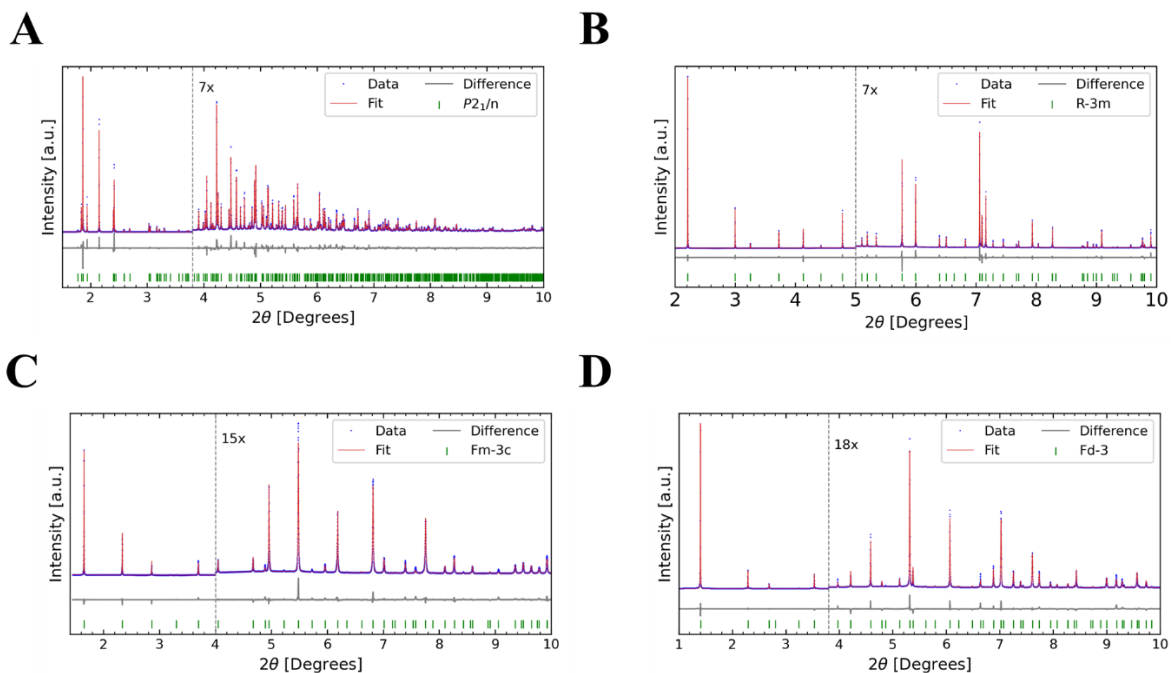


Figure S1: Rietveld refinement at 0 bar of A- Si-STT (Rwp: 6.256 %, Rp: 6.309 %, Rexp: 1.41 %), B- Si-CHA (Rwp: 7.381 %, Rp: 4.714 %, Rexp: 1.355 %), C- Na-LTA (Rwp: 7.212 %, Rp: 5.758 %, Rexp: 2.128 %), and D- Na-FAU (Rwp: 7.104 %, Rp: 5.362 %, Rexp: 1.055 %) at 298K (blue: experimental; red: calculated; grey: difference, $\lambda = 0.354180(1)$ Å).

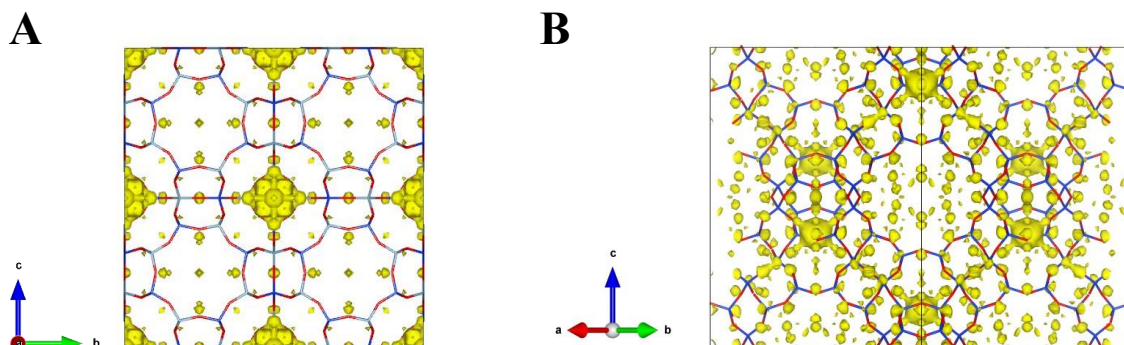


Figure S2: Fourier difference map for Na-LTA (A) and Na-FAU (B), evidencing remaining water in the pores as residual electronic density.

Table S5: Interaction between the oxygen atoms of specific sites and either the cations, the framework oxygen atoms, or those from water molecules.

	Omol12	Omol13	Omol22	Omol23
Na-LTA	Na2: 2.55-3.06 Ow3: 2.93 Ow5: 2.665-2.93	Na1: 2.80 Ow5: 2.576-2.972		
Na-FAU	Na3: 2.796 OW6: 3.038	OW6: 2.781 O4: 2.845	Na2: 2.704 Na3: 2.906-2.931 OW6: 3.03	Na3: 2.988 OW6: 2.527

Computational methodology

1. Adsorbent and adsorbate microscopic models

The atomic positions for the investigated zeolites were taken from the IZA database [1]. Table S5 summarizes the main features of the simulation boxes for each investigated zeolite structure. Si-CHA and Si-STT zeolite structures were simulated under their purely silicate chemical composition (SiO_2), whereas Na-LTA and Na-FAU in aluminosilicated, charge compensating cations containing forms. In these two latter structures, Al atoms were distributed along the framework with respect to the Löwenstein rule. The zeolite systems are assumed to be semi-ionic, and the partial charge carried by zeolite atoms are detailed in Table S6. The CO_2 molecules were described using the TrePPE-EH model [2], considering the CO_2 molecule as rigid, with CO bond length equals to 1.16 Å. Finally, H_2O molecules were described using the five-site model, TIP5P, able to accurately reproduce liquid water density [3]. Within the frame of this model, positive electrostatic charges are beared by hydrogen atoms, whereas negative ones by lone-pair interaction sites, designed as L. The model assumes the geometry of the molecule fixed, with OH bond length of 0.9572 Å and HOH bond-angle of 104.52°.

Table S6: Chemical composition and size of the simulation boxes used in the GCMC.

Zeolite structure	Si-STT	Si-CHA	Na-LTA	Na-FAU
Unit cell chemical composition	$\text{Si}_{256}\text{O}_{512}$	$\text{Si}_{256}\text{O}_{512}$	$\text{Na}_{96}\text{Si}_{96}\text{Al}_{96}\text{O}_{384}$	$\text{Na}_{92}\text{Si}_{100}\text{Al}_{92}\text{O}_{384}$
Unit cell dimensions a^*b^*c $\alpha^* \beta^* \gamma$	26.100 21.853 27.146 90 102.91 90	27.036 27.036 29.063 90 90 120	24.555 24.555 24.555 90 90 90	25.028 25.028 25.028 90 90 90
Simulation box constitution (nb of UC in each direction)	2 x 1 x 2	2 x 2 x 2	1 x 1 x 1	1 x 1 x 1

2. The zeolite/adsorbate interaction potential

The intermolecular adsorbate/adsorbate and adsorbate/zeolite interactions were modeled using a sum of the repulsion-dispersion and the electrostatic potential expressed via the Lennard-Jones (LJ) and the Coulombic terms, as described in Equation S1:

$$U_{ij}^{\text{Inter}} = 4\varepsilon_{ij}[(\frac{\sigma_{ij}}{r_{ij}})^{12} - (\frac{\sigma_{ij}}{r_{ij}})^6] + \frac{q_i q_j}{4\pi\varepsilon_0 r_{ij}} \quad (\text{S1})$$

where q_i and q_j are the electrostatic sites partial charges, r_{ij} is the distance separating two interacting sites, and ε_{ij} and σ_{ij} are the corresponding LJ interatomic potential parameters. The LJ interatomic parameters as well as the partial atomic charges for both, purely siliceous and aluminosilicated zeolites were taken from the Clay force field [4]. Whereas a LJ interaction site is placed on each atom of the CO₂ molecule in the Trappe-EH model [2], in the TIP5P model of water molecule solely oxygen atoms constitute LJ interaction sites. The whole set of all applied parameters is reported in Table S7. Finally, the cross-term Lennard-Jones parameters were calculated through the Lorentz-Berthelot mixing rule. The refined and simulated occupancies of sodium cation sites in Na-LTA and Na-FAU are summarized in Table S8.

Table S7: Lennard-Jones (ε , σ) parameters and partial atomic charges (q) carried by zeolite and CO₂ molecules, as a function of the chemical composition of the zeolite.

Atom	ε/k_B (K)	σ (Å)	$q(e)$
C(CO ₂)	27.0	2.80	0.70
O(CO ₂)	79.0	3.05	-0.35
O (SiO ₂ zeolite)	78.20	3.17	-1.05
Si (zeolite)	0.93×10^{-3}	3.30	2.10
O (AlSi zeolite)	78.20	3.17	-1.165
Al (Na-FAU)	0.93×10^{-3}	3.30	1.78
Al (Na-LTA)	0.93×10^{-3}	3.30	1.76
Na ⁺	65.47	2.35	0.80
H(H ₂ O)	0	0	0.241
O(H ₂ O)	80.52	3.12	0
L(H ₂ O) (lone pair interaction site)	0	0	-0.241

Table S8: Comparaison of Na⁺ site occupancies in Na-LTA and Na-FAU from Rietveld refinement and simulation.

	Na-LTA		Na-FAU		
Site Na ⁺	I	II	I'	II	III'
Occupancy from refinement	1	0.33	0.81	1	0.29
Occupancy from simulation	1	0.33	0.71	0.98	0.39

3. Grand Canonical Monte Carlo (GCMC) simulation

Absolute adsorption isotherms of CO₂ were simulated in the purely silicated Si-STT and Si-CHA zeolites and the cationic Na-LTA and Na-FAU zeolites, at the temperature of 298 K. For that purpose, we have applied the GCMC method [5], implemented within the 8.2.3 version of the Towhee code [6]. These simulations consisted of evaluating the average number of carbon dioxide molecules whose chemical potential values equal those of the bulk phase for a given pressure and temperature. Beforehand, a MC simulation in the NpT ensemble was applied to calculate the chemical potential through the Widom method [5]. Several previous studies have shown the necessity of relaxing the charge-compensating cations during the GCMC simulation of adsorption to correctly sample the configurational space [7]. Consequently, while keeping the framework rigid (Si, Al, and zeolite O atoms), the extra-framework cations were allowed to displace. The system was first equilibrated during a period of 1.10^7 MC steps and the subsequent period of 2.10^7 MC steps was used for the production phase. We employed the following MC moves: CO₂ molecule creations and deletion, CO₂ molecule center of mass translation and center of mass rotation, CO₂ molecule and sodium cation intra-box swap move, and sodium cation translation. In simulations with fixed number of H₂O molecules, we additionally applied translation, rotation and intra-box swap moves to water molecules. The maximum displacements for translation and rotation moves were adjusted to yield an acceptance rates close to 50%. The periodic conditions were applied in all directions of the space. The Ewald summation technique was used in the calculation of the long-range electrostatic interactions. A short-range repulsion–dispersion interaction cut-off of 12.5 Å was applied. Furthermore, as the CO₂ molecule kinetic diameter is higher (~3.3 Å) than the one of the six-membered ring window of the sodalite cages (~2.2 Å), carbon dioxide cannot access the sodalite cages [8]. Consequently, in our simulations, access to sodalite cages was prohibited for CO₂ molecules and allowed for water molecules. Finally, in order to study the structure of the adsorbed CO₂ molecules, in presence and absence of water molecules, we performed MC simulations in ensemble NVT and we have recorded the CO₂, Na⁺ and H₂O configurations every 1000 steps during the MC runs. These configurations were subsequently used to report the radial distribution functions for sodium cations in various crystallographic sites and oxygen atoms of the CO₂ molecule (Fig. S3) as well as the cumulated snapshots, showing the CO₂ molecules' localizations.

We have achieved complementary NVT-MC simulations for the saturation loading (20 bar) in all studied structures. Thus, we could determine the site occupation factors for each experimentally identified CO₂ crystallographic site. These results are summarized in Table S9, which presents the site-specific occupancies derived from the simulations, allowing direct comparison with experimental data.

Table S9: Comparaison CO₂ site occupancies for each zeolite from Rietveld refinement and NVT-MC simulation.

		Si-STT	Si-CHA	Na-LTA	Na-FAU
Site occupancy of mol1	From refinement	0.82	0.36	0.29	0.4
	From simulation	0.97	0.34	0.28	0.27
Site occupancy of mol2	From refinement	0.72	0.34		0.38
	From simulation	0.66	0.55		0.35
Site occupancy of mol3	From refinement	0.65			
	From simulation	0.69			
Site occupancy of mol4	From refinement	0.76			
	From simulation	0.70			

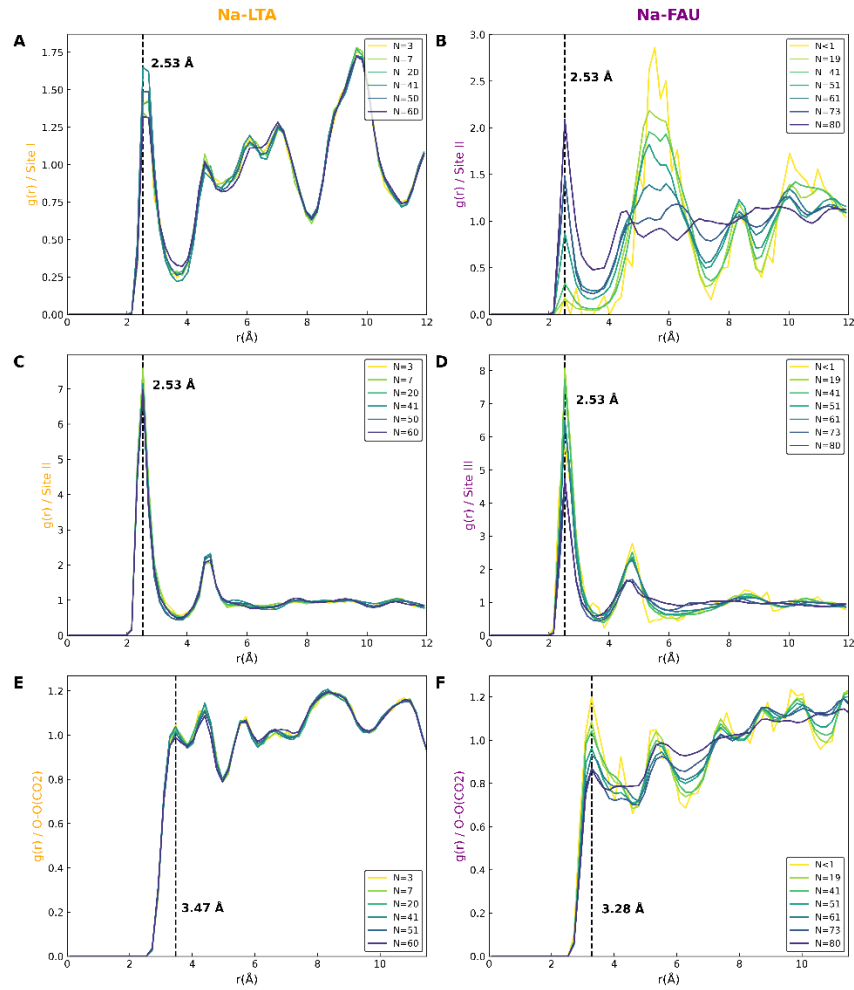


Figure S3: RDFs for oxygen atom of the CO₂ and sodium cations for Na-LTA (A, C), Na-FAU (B, D), and oxygen atom of the framework and oxygen atom of the CO₂ for Na-LTA (E) and Na-FAU (F). N represents the number of CO₂ molecules present in each simulation.

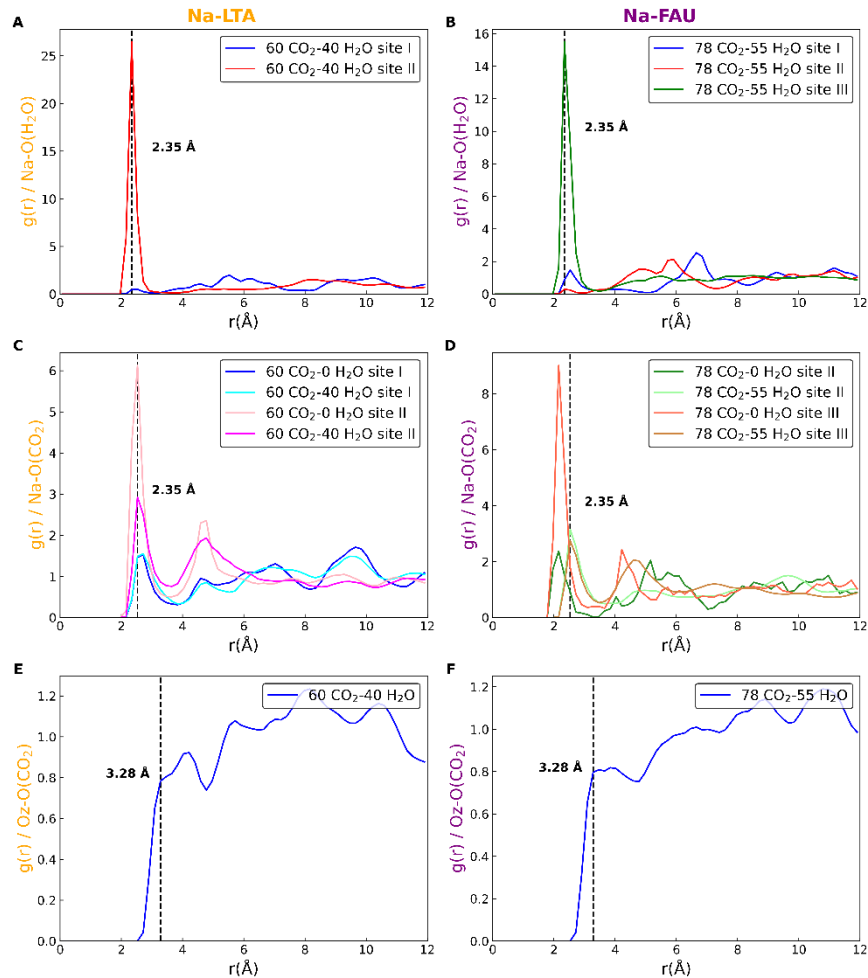


Figure S4: RDFs for oxygen atom of the CO₂ and sodium cations for Na-LTA (A, C), Na-FAU (B, D), and oxygen atom of the framework and oxygen atom of the CO₂ for Na-LTA (E) and Na-FAU (F) in the presence of water. The experimental condition, defined by the number of CO₂ and H₂O molecules, is indicated in the legend.

In-situ crystallographic study

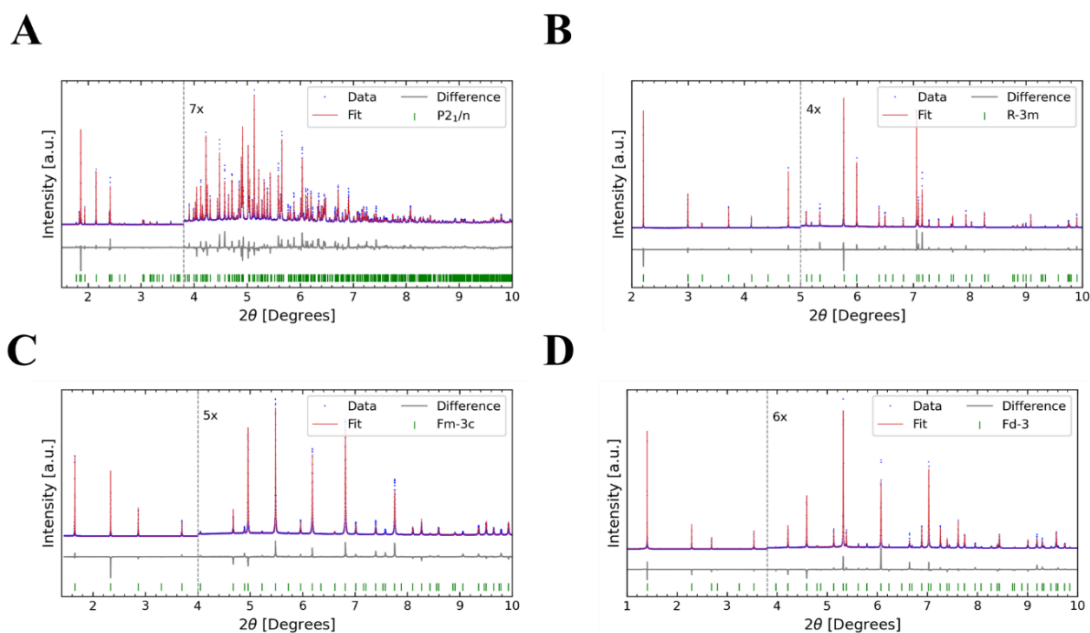


Figure S5: Rietveld refinement at 20 bar of A- Si-STT (Rwp: 7.875 %, Rp: 6.828 %, Rexp: 1.349 %), B- Si-CHA (Rwp: 7.726 %, Rp: 5.212 %, Rexp: 1.303 %), C- Na-LTA (Rwp: 8.359 %, Rp: 6.329 %, Rexp: 2.006 %), and D- Na-FAU (Rwp: 7.458 %, Rp: 5.665 %, Rexp: 1.003 %) at 298K (blue: experimental; red: calculated; grey: difference, $\lambda = 0.354180(1)$ Å).

CO₂ parametric refinements and isotherm fitting

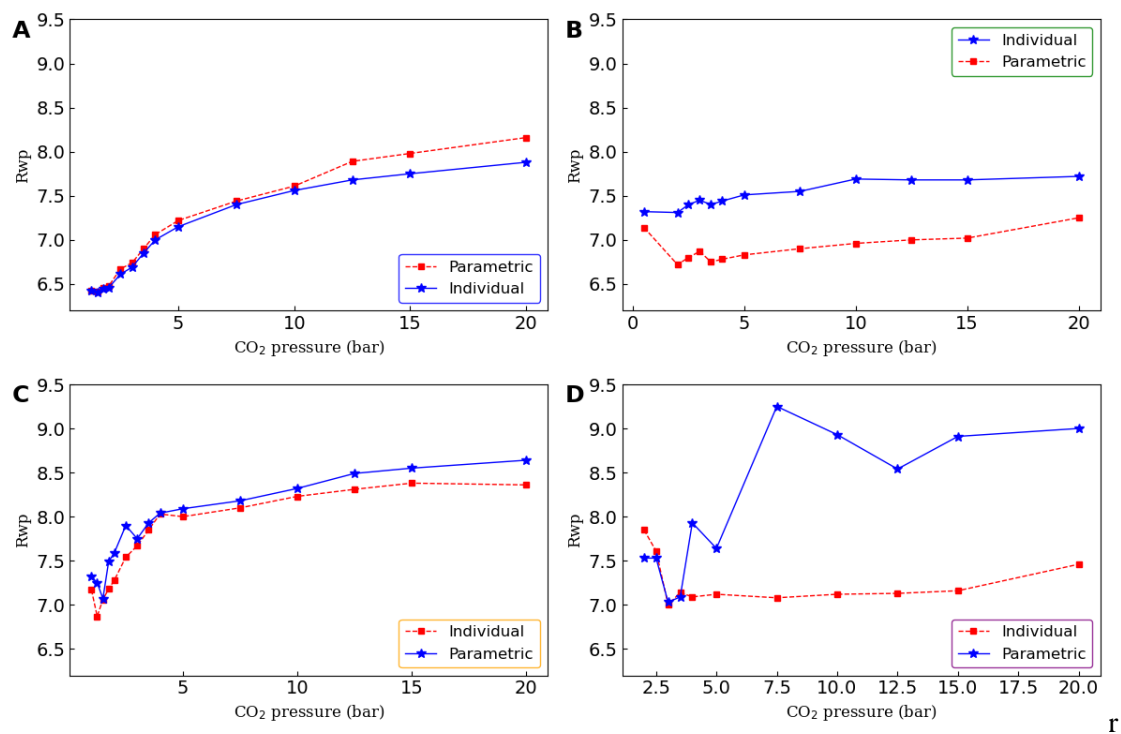


Figure S6: Evolution of Rwp for Rietveld refinement compared to parametric refinement for (A) Si-STT, (B) Si-CHA, (C) Na-LTA, and (D) Na-FAU.

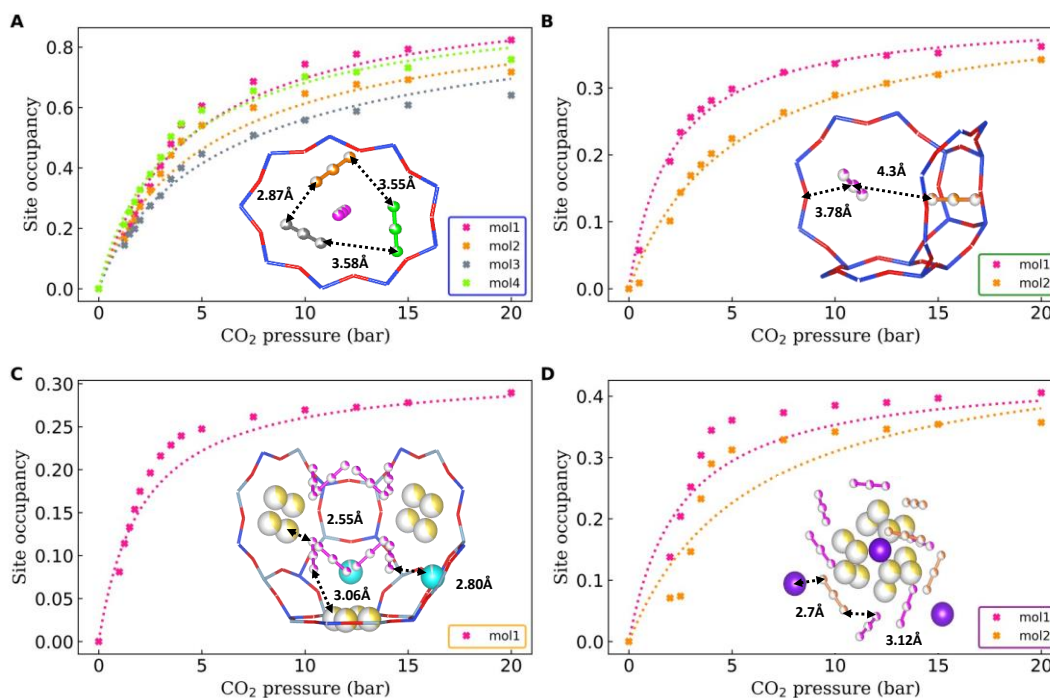


Figure S7: The evolution of the different sites as a function of CO₂ loading pressure, obtained from parametric refinements (dotted lines) and from classic refinements (cross markers), is also shown for comparison. The crystallographic model of each zeolite at 20 bar is also displayed in each subplot. A – Si-STT; B – Si-CHA; C – Na-LTA; D – Na-FAU.

References

- [1] Database of Zeolite Structures, <http://www.iza-structure.org/databases/> (accessed on 10 November 2024).
- [2] J. Potoff and J. Ilja Siepmann, *AIChE Journal*, 2001, **47**, 1676–1682.
- [3] M.W. Mahoney and W.L. Jorgensen, *J. Chem. Phys.*, 2000, **112**, 8910–8922.
- [4] R. Cygan, J. Liang and A. Kalinichev, *The Journal of Physical Chemistry B*, 2004, **108**, 1255–1266.
- [5] D. Dubbeldam, A. Torres-Knoop and K. Walton, *Mol. Simul.*, 2013, **39**, 1253–1292.
- [6] M. Martin, *Mol. Simul.*, 2013, **39**, 1212–1222.
- [7] J. Castillo, J. Silvestre-Albero, F. Rodriguez-Reinoso, T. Vlugt and S. Calero, *Physical Chemistry Chemical Physics*, 2013, **15**, 17374–17382.
- [8] G. Maurin, P. Llewellyn and R. Bell, *The Journal of Physical Chemistry B*, 2005, **109**, 16084–16091.